Catalytic decomposition performance for O_3 and NO_2 in humid indoor air on a MnO_x/Al_2O_3 catalyst modified by a cost-effective chemical grafting method

Longwen Chen*, Michel Ondarts, Jonathan Outin, Yves Gonthier, Evelyne Gonze

Université Grenoble Alpes, Université Savoie Mont Blanc, CNRS, Laboratoire d'Optimisation de la Conception et Ingénierie de l'Environnement (LOCIE), 73000 Chambéry, France

ARTICLE INFO

ABSTRACT

Processes based on non-thermal plasma (NTP) for indoor air treatment inevitably lead to the formation of toxic by-products such as ozone (O_3) and nitrogen oxides (NO_x). Adding a step of heterogeneous catalysis in series with NTP could allow for the decomposition of the by-products. Therefore, different catalysts were developed based on transition metal oxides, such as NiO_x, CoO_x and MnO_x with different weight percentage 1, 5 and 10 wt.%, deposited on a γ-Al_2O_3 support. The O_3 removal efficiency (ORE) and the NO_x removal efficiency (NRE) were very encouraging in dry air: about 65% and 80%, respectively, by using 2 g 5 wt.% MnO_x/Al_2O_3 catalyst under the experimental conditions. However, strongly negative effects of relative humidity (RH) on the catalytic decomposition performance were observed. To overcome this limitation, the catalyst surface was modified to make it hydrophobic using a cost-effective chemical grafting method. This treatment consisted in impregnating the 5 wt.% MnO_x/Al_2O_3 catalyst with different trichloro(alkyl)silanes (TCAS). The effects of different linker lengths and amounts of TCAS for the hydrophobicity and the decomposition performance of surface-modified catalysts under humid conditions were investigated. Our results show that the surface-modified catalyst with the shortest linker and 0.25 mmol/g_{cat} of modifying agent represents the best catalytic decomposition performance for O_3. Its ORE is 41% at 60% RH, which is twice that of the non-modified catalyst.

© 2017 The Research Center for Eco-Environmental Sciences, Chinese Academy of Sciences. Published by Elsevier B.V.

Introduction

Clean air is considered to be a basic requirement for human health and well-being. Indoor air quality (IAQ) has become a public health concern as people spend an average of 80% to 90% of their time in indoor environments, such as homes, work-places, schools, shops, *etc.* (Qualité de l'air intérieur, ANSES). Studies by the United States Environmental Protection Agency (US EPA) on human exposure to air pollutants indicate that the level of many pollutants in indoor air may be two to five times, and occasionally more than 100 times, higher than the level in outdoor air (Carver et al., 2010). Therefore, the elimination of indoor air pollutants is an important scientific topic and much research is being carried out in this area to develop more efficient, environmentally friendly and low-energy consumption processes. Conventional technologies for indoor air treatment are physical adsorption, thermal and catalytic oxidation and photo-catalytic processes (Magureanu et al., 2005).

* *Corresponding author. E-mail:* longwen.chen@univ-smb.fr (Longwen Chen).

However, these technologies have limitations related to their low energy efficiency (Subrahmanyam et al., 2006). In addition, for many applications, particularly in the removal of very dilute concentrations of indoor air pollutants, conventional technologies are not satisfactory (Mista and Kacprzyk, 2008). This would be another important restriction to their application in indoor environments, where, for example, the volatile organic compound (VOC) concentration is on the order of hundreds of ppb or even tens of ppb (Kirchner et al., 2006).

In this context, processes based on non-thermal plasma (NTP) or cold plasma represent an innovative and alternative method for indoor air treatment (Ondarts et al., 2017; Thevenet et al., 2014; Van Durme et al., 2008). Indeed, implemented under a suitable configuration such as an electrostatic precipitator (ESP), NTP can achieve multiple purification effects in indoor air treatment processes, including particulate matter trapping, sterilization, as well as VOC removal (Byeon et al., 2010). However, as NTP takes place in air, the formation of ozone (O_3) and nitrogen oxides (NO_x), which are considered as toxic by-products and can be more harmful than the primary compounds, is unavoidable. Hazardous O_3 as a primary by-product in NTP is always a major concern for indoor NTP devices. O_3 and its oxidizing derivatives can react with organic compounds in indoor air and produce VOC. Because of its toxicity, the World Health Organization (WHO) has set the maximum human allowable exposure concentration of O_3 for an 8-hr period at 100 $\mu g/m^3$ (about 0.05 ppm) (World Health Organization, 2000). Long-lived NO_x such as nitric oxide (NO) and nitrogen dioxide (NO_2) are also toxic by-products formed in NTP. NO_x can react with water vapor or other compounds present in air to form nitric acid vapor. The WHO has proposed a NO_2 guideline value of 40 $\mu g/m^3$ as an annual mean and 200 $\mu g/m^3$ as an 1-hr mean (World Health Organization, 2000). The formation of by-products leads to considerable restrictions in the practical application of NTP for indoor air pollution control. In the previous study, we investigated O_3 and NO_x formation in NTP for different conditions (Fig. 1) (Ondarts et al., 2017). Our results show that the concentration of NO_2 in negative corona is significantly lower than that of O_3. For the same operating conditions, the maximum concentration of NO_2 (0.05 ppm) is only 0.6% of the concentration of O_3 (8.9 ppm). For this reason, the present study places more emphasis on O_3 when referring to the catalyst

selection for O_3 and NO_2 decomposition. Besides, negligible NO is formed in negative corona. Consequently, in this study we assume the approximation [NO_2] (NO_2 concentration) $\approx$ [NO_x] (NO_x concentration).

In the early 2000s, researchers began to investigate the combination of NTP and heterogeneous catalysis, which seemed possible to avoid the drawback of NTP alone and to develop more efficient and energy-saving processes with a reinforcement of pollutant removal efficiency (Van Durme et al., 2007). The subject of catalytic decomposition for O_3 has been reviewed by Dhandapani and Oyama (1997). Two groups of catalytic materials are generally used for O_3 decomposition in ambient conditions: noble metal catalysts, mainly Pt and Pd, and catalysts based on transition metal oxides such as Mn, Co, Cu, Fe, Ni and Ag (Dhandapani and Oyama, 1997). The latter are usually deposited on materials with a large specific surface area, such as Al_2O_3, TiO_2, SiO_2, zeolite, activated carbon, or a combination of both (Heisig et al., 1997). Noble metal catalysts are characterized by good stability and high activity at relatively low temperatures (Everaert and Baeyens, 2004). However, their high costs, sensitivity to poisoning by chemical compounds, and formation of toxic polychlorinated compounds when used for the oxidation of chlorinated VOC have necessitated research on alternative catalysts. By contrast, catalysts based on transition metal oxides are far less expensive and more resistant to poisoning of by-products. In some cases, they exhibit a catalytic activity comparable to that of noble metal catalysts. As a catalyst support, γ-Al_2O_3, the most porous and with the largest specific surface area among different alumina, has a very wide range of applications in industry and in the laboratory. Furthermore, its high erosion resistance can ensure a longer catalyst life (Van Durme et al., 2009).

Dhandapani and Oyama (1997) investigated the decomposition of O_3 by different catalysts based on transition metal oxides deposited on γ-Al_2O_3. According to the results, MnO_2 showed the highest catalytic activity with an O_3 removal efficiency (ORE) of 42% followed by Co_3O_4 (39%), NiO (35%) and Fe_2O_3 (24%). Moreover, Guo et al. (2006) demonstrated that the MnO_x catalyst exhibited the best performance in terms of O_3 decomposition, followed by CoO_x. However, Long et al. (2011) obtained a better ORE with NiO than MnO_2. These differences may be due to the different operating and environmental
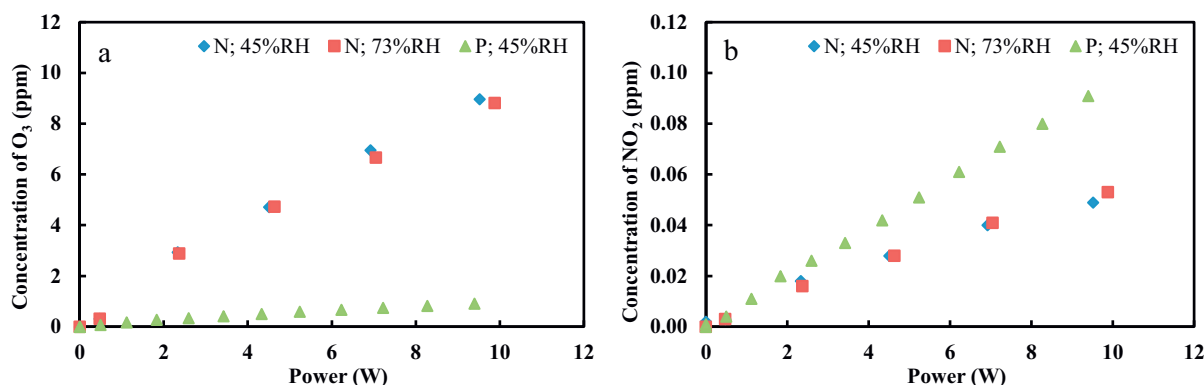
Fig. 1 – Concentrations of (a) O_3 and (b) NO_2 measured at the outlet of the non-thermal plasma (NTP) as a function of dissipated power under negative (N) and positive (P) voltage with different relative humidity (RH) (45% and 73%).

conditions. All in all, oxides of manganese, cobalt and nickel are indeed transition metal oxide catalysts with the best decomposition performance for O_3. Transition metal oxide catalysts have also been reported to be highly effective for NO_x removal in the presence of O_3 (Guo et al., 2006; Niu et al., 2006). Guo et al. (2006) showed a NO_x removal efficiency (NRE) trend with different transition metal oxide catalysts: CuO has the best NRE, followed by CoO_x and MnO_x. MnO_x has the best catalytic activity for O_3 decomposition, but its NO_x outlet concentration is the highest among all tested catalysts. This is probably due to the fact that with a MnO_x catalyst, most O_3 is decomposed to O_2 and O, which may combine with nitrogen atoms and generate more NO_x compared with other catalysts (Guo et al., 2006). Furthermore, Lin et al. (2016) studied the catalytic deep oxidation of NO_x by O_3 over MnO_x/Al_2O_3 catalyst. The authors found that the NO_2 concentration was reduced from 600 to 100 ppm with an O_3 leakage of less than 20 ppm by applying MnO_x/Al_2O_3, which has an appreciable catalytic activity for both O_3 and NO_x degradation.

The amount of deposited transition metal oxides has an important effect on the decomposition performance of the catalyst. Rezaei et al. (2013) investigated the oxidation of toluene in the presence of O_3 with four different weight percentages (wt.%) of MnO_x/Al_2O_3 catalyst (1, 5, 10 and 20 wt.%). Experimental results showed that a lower weight percentage of MnO_x/Al_2O_3 has a higher catalytic activity for toluene oxidation. This phenomenon was confirmed by other authors. Wang et al. (2014) found that 1.1 wt.% MnO_x has a better decomposition performance for O_3 than that of the 11 wt.% catalyst, whose lower catalytic activity is mainly due to the more compact structural morphology. In addition, Wang et al. (2016) demonstrated that 6 wt.% MnO_x/Al_2O_3 is the optimal weight percentage for o-xylene conversion among the different ones tested (2, 4, 6, 8 and 10 wt.%). Therefore, three different weight percentages of transition metal oxides (1, 5 and 10 wt.%) were proposed in this study for catalyst preparation.

Like many other catalysts, the presence of water vapor may limit the catalytic activity of Al_2O_3-supported catalysts, especially for high relative humidity (RH). As a ceramic material made from metal oxide, Al_2O_3 is hydrophilic in nature owing to the presence of hydroxyl groups on its surface (Kujawa et al., 2015). Numerous studies have investigated the effects of RH on the decomposition performance of Al_2O_3-supported catalysts (Einaga and Futamura, 2006; Fan et al., 2010; Li et al., 2011). Owing to the hydrophilicity of Al_2O_3, water molecules can cover the catalyst and poison it by occupying the active sites on the surface. Besides, the competition of water molecules with

pollutant molecules for adsorption on the active sites can effectively reduce the catalytic activity. In this way, water vapor can considerably inhibit the processes of O_3 decomposition and other pollutants oxidation on the catalyst surface. However, some studies show that, the presence of a small amount of water vapor can improve the catalyst performance in the elimination of some pollutants (e.g., VOC). Einaga and Futamura (2006) have reported that a RH of 0.7% can suppress the deactivation of MnO_x/γ-Al_2O_3 catalyst in benzene oxidation, by promoting the oxidation of organic byproducts on the catalyst surface.

The hydrophilic surface of alumina can be changed to a hydrophobic property by a surface modification treatment (Esmaeilirad et al., 2016; Kujawa et al., 2014) that is often utilized to increase the hydrophobicity of ceramic material by either introducing radical groups or hydrophobic polymer chains on the surface (Kujawa et al., 2013). Hydrophobization of ceramic surfaces can be done using various methods. However, compounds with a reactive group should always be used (e.g., methoxy, ethoxy, or active chlorine) (Kujawa et al., 2013; Paul et al., 2011). Organosilanes such as methylsilanes, linear alkylsilanes, aromatic silanes, and perfluorinated alkylsilanes are the most widely used materials for hydrophobic surface modification (Esmaeilirad et al., 2016). In comparison with the most commonly used modifying agents such as perfluoroalkylsilanes and other typical modifiers, linear alkylsilanes such as trichloro(alkyl)silanes (TCAS) are much cheaper and can also create a physically and thermally stable hydrophobic surface (Esmaeilirad et al., 2016). In fact, TCAS possess three major parts: an organo-functional group, a linker and hydrolysable groups, which can be hydrolyzed and condensed to oligomers during the modification process. Eventually, stable covalent bonds are created between the hydrolysable groups of the modifying agent and the hydroxyl groups on the substrate (Esmaeilirad et al., 2016). Therefore, the presence of an aliphatic hydrocarbon substituent can effectively change the surface character of a ceramic material from hydrophilic to hydrophobic (Fig. 2). Esmaeilirad et al. (2016) used TCAS as modifying agent for aluminum alloy surface modification. The authors found that the super-hydrophobic properties of the aluminum alloy surface increase by using a longer linker and a greater amount of TCAS. However, a longer linker and a greater amount of modifying agent probably lead to a more significant steric hindrance effect, which can greatly prevent the access of gaseous molecules to the catalyst surface and their contact with active components. Hence, a compromise between the hydrophobic property and the decomposition performance
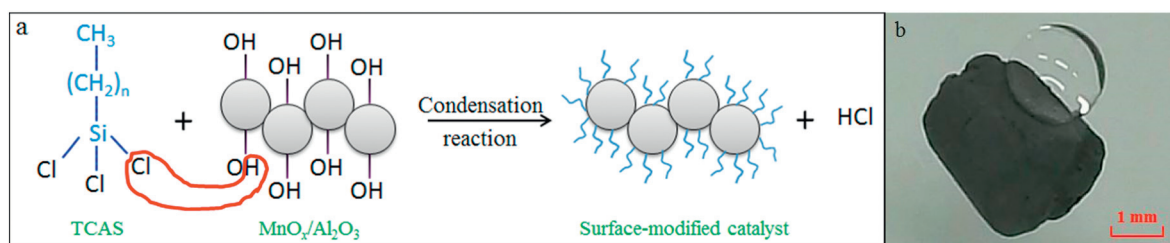

Fig. 2 – (a) Chemical grafting process and (b) hydrophobic behavior of the surface-modified catalyst illustrated by the water droplet shape. TCAS: trichloro(alkyl)silanes.

of the catalyst was considered in this study, in which the latter was given priority.

In the present study, the first objective was to develop a catalyst with the best decomposition performance for O_3 and NO_x formed in NTP. Therefore, a series of supported transition metal oxide catalysts were prepared by the vacuum impregnation method and then tested under a range of operating and environmental conditions. Furthermore, a facile, practical and cost-effective chemical grafting method for catalyst surface modification was carried out by using different modifying agents of TCAS, in order to improve the hydrophobicity and the decomposition performance of catalysts in humid indoor air. Finally, the effects of different linker lengths and amounts of modifying agent for the hydrophobicity and the catalytic activity were investigated by establishing the adsorption isotherms of water/materials, analyzing the catalyst structure and comparing the ORE and NRE between surface-modified and non-modified catalysts.

1. Materials and methods

1.1. Experimental set-up

The experimental set-up is shown in Fig. 3. It consists of three parts: generation of clean air, ESP and a fixed-bed catalytic reactor (FCR). Experiments were conducted in continuous flow mode. Compressed air was used as carrier gas and its flow rate (150 ± 2 L/min) was controlled by a mass flow controller (GFC67, Aalborg, USA). The carrier gas was cleaned and dried

by passing successively through an oil separator, a desiccant cartridge, an activated carbon filter and a particulate filter. According to the required RH (<2% to 65%), a part of the air flow was humidified and saturated by a temperature-controlled water bubble column. Dry air and humid air were then mixed in a mixing chamber to obtain zero air flow before being introduced into the ESP, in which direct current (DC) corona discharge was generated. The wire-cylinder ESP consisted of an outer steel cylinder (20 mm in inner diameter, 20 cm in length) connected to the ground, and a central discharge electrode wire in tungsten (0.125 mm in diameter). A high-voltage power supply (SR10-P-300, Technix, France) was used to apply a varying negative voltage (0–10 kV) to the central discharge electrode, in which negative corona was thus created by a non-uniform electrical field. The temperature and RH were continuously measured upstream and downstream of ESP, by using type K thermocouples and capacitive hygrometers (TH300, Kimo, France), respectively, both connected to a data-acquisition unit. According to different operating and environmental conditions in this study, the ESP generated about 6 to 8 ppm and 0.15 to 0.18 ppm of O_3 and NO_2, respectively. The sample gas at the ESP outlet was then introduced by an air compressor into the FCR, which was in the form of a cylindrical column. This FCR was made of PMMA with an internal diameter of 24 mm, in which 2 g catalyst was deposited on a stainless mesh bed. The gas flow rate (5.00 ± 0.05 L/min) in the FCR was also controlled by a mass flow controller (GFC17, Aalborg, USA) and a three-way valve allowed the sample gas to be taken either at the inlet or at the outlet of the FCR for the downstream monitors.
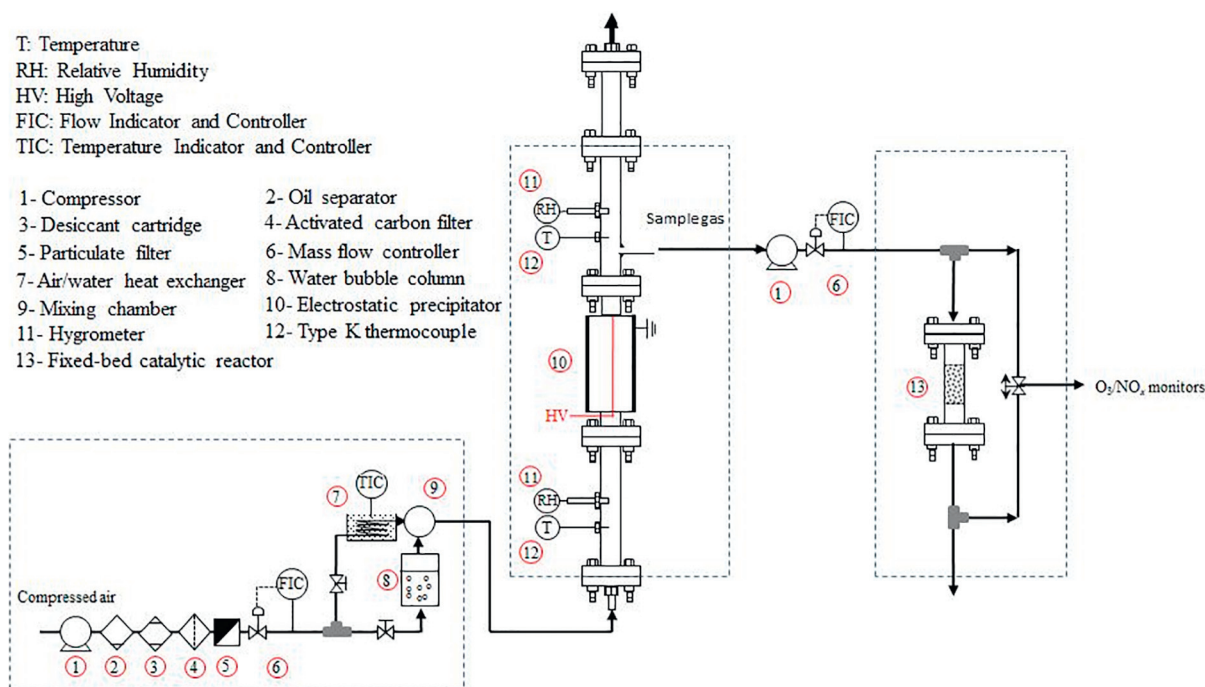

T: Temperature
RH: Relative Humidity
HV: High Voltage
FIC: Flow Indicator and Controller
TIC: Temperature Indicator and Controller

1- Compressor
2- Oil separator
3- Desiccant cartridge
4- Activated carbon filter
5- Particulate filter
6- Mass flow controller
7- Air/water heat exchanger
8- Water bubble column
9- Mixing chamber
10- Electrostatic precipitator
11- Hygrometer
12- Type K thermocouple
13- Fixed-bed catalytic reactor

Fig. 3 – Schematic of the experimental set-up.

1.2. Analytical methods

Concentration measurements were conducted in continuous flow mode at the inlet and at the outlet of the FCR. The O_3 concentration was continuously quantified by an ultraviolet photometric O_3 monitor (APOA-370, Horiba, France) for a concentration range from 0 to 1 ppm. The detection threshold is 0.5 ppb with a measurement accuracy of ±1.0% of full scale. Since a few ppm of O_3 is required to investigate the decomposition performance of a catalyst, a simple dilution system was implemented. This system uses ambient air to dilute the O_3 concentration in the sample gas, before being introduced into the O_3 monitor. The flow rate of both the sample gas and ambient air is controlled by a mass flow controller. These two mass flow controllers allow the percentage between the sample gas and ambient air to be accurately distributed, so that the dilution factor can be determined. NO_x concentrations were also continuously quantified *via* chemiluminescence using a NO_x monitor (APNA-370, Horiba, France) for a concentration range from 0 to 1 ppm with a measurement accuracy of ±1.0% of full scale and a detection threshold of 0.5 ppb.

1.3. Catalyst preparation

In this study, we have chosen γ-Al_2O_3 (N°414069, Sigma-Aldrich, USA) as catalyst support. The following catalyst precursors were used: manganese(II) nitrate tetrahydrate ($Mn(NO_3)_2 \cdot 4H_2O$) (N°63547, Sigma-Aldrich, USA), cobalt(II) nitrate hexahydrate (Co$(NO_3)_2 \cdot 6H_2O$) (N°239267, Sigma-Aldrich, USA), and nickel(II) nitrate hexahydrate (Ni$(NO_3)_2 \cdot 6H_2O$) (N°72253, Sigma-Aldrich, USA). For the catalyst surface modification treatment, trichloro(methyl)silane (TCMS) (N°M85301, Sigma-Aldrich, USA), trichloro(octyl)silane (TCOS) (N°235725, Sigma-Aldrich, USA), and trichloro(octadecyl)silane (TCODS) (N°104817, Sigma-Aldrich, USA) were chosen as modifying agents. Their simplified molecular structural formulas are presented in Fig. 4.

1.3.1. Vacuum impregnation method
Supported transition metal oxide catalysts were prepared through the vacuum impregnation method by introducing an appropriate mass of manganese, cobalt or nickel precursor element into the γ-Al_2O_3 extruded cylinders, and the obtained catalysts were designated as MnO_x/Al_2O_3, CoO_x/Al_2O_3 and NiO_x/Al_2O_3, respectively. A nominal loading amount of precursor is based on the mass of the metallic element per mass of the catalyst (support plus metallic element). Three different precursor loading amounts (1, 5 and 10 wt.%) were therefore used to prepare the catalysts. Firstly, a vacuum environment (10^{-2} mbar) in a two-neck flask containing γ-Al_2O_3 cylinders was achieved thanks to a vacuum pump. Then the valve between the flask and the column was opened to pour the precursor solution onto γ-Al_2O_3. Subsequently, the mixture was oven-dried at 80°C for 24 hr and then calcined in a muffle roaster. The calcination temperature and time depend on the chemical properties of different precursor elements. For example, the mixture of manganese nitrate and γ-Al_2O_3 was calcined at 500°C for 6 hr to form a major MnO_2 crystalline structure over the catalyst (Heisig et al., 1997; Long et al., 2011; Radhakrishnan and Oyama, 2001a; Rezaei et al., 2013; Rezaei and Soltan, 2012), which is considered to have the best catalytic activity for O_3 decomposition (Dhandapani and Oyama, 1997). Besides, calcinations at 600°C for 5 hr and for 4 hr were carried out in order to form NiO_x/Al_2O_3 and CoO_x/Al_2O_3, respectively. Finally, supported transition metal oxide catalysts with different weight percentages of precursor element were obtained.

1.3.2. Chemical grafting method
Each experiment consisted in adding a precise quantity of modifying agent (in mmol) to the given amount of 5 wt.% MnO_x/Al_2O_3 catalyst (in grams). Three different kinds (TCMS, TCOS and TCODS) and four different ratios (Q = 0.25, 0.5, 1 and 2 mmol/g_{cat}) of modifying agents were used to carry out this surface modification process. Initially, MnO_x/Al_2O_3 was immersed in ethanol for 6 hr and oven-dried at 110°C for 2 hr. Then, catalysts were impregnated in different modifying agent-hexane solutions for 24 hr at room temperature, which were pre-prepared by the corresponding amount of modifying agent, according to the catalyst mass used. Resultant samples were then oven-dried at 150°C for 2 hr. Finally, MnO_x/Al_2O_3 surface-modified catalysts with different grafted modifying agents were obtained; which are denoted as M-modifying agent-Q. For example, MnO_x/Al_2O_3 surface-modified catalyst, by using TCOS as modifying agent with a ratio Q of 0.5 mmol/g_{cat}, is denoted as M-TCOS0.5.

1.4. Water vapor sorption isotherm

ISO 12571 was used as a reference standard to determine the water vapor sorption isotherms of different catalysts (ISO, 2013). Before testing, samples were oven-dried at 100°C to
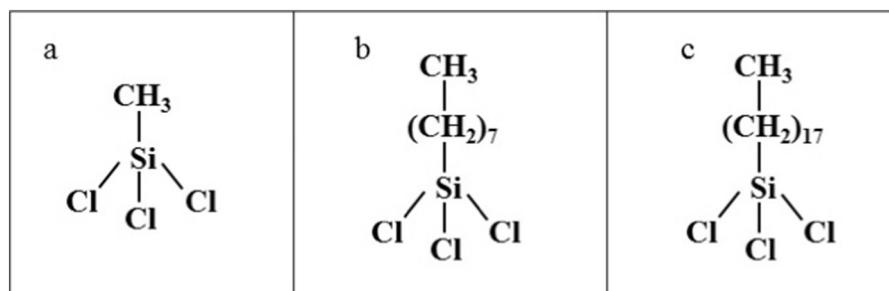

Fig. 4 – Simplified molecular structural formulas of (a) trichloro(methyl)silane (TCMS), (b) trichloro(octyl)silane (TCOS), and (c) trichloro(octadecyl)silane (TCODS).

constant mass. Samples were then placed consecutively in a series of seven environments at different increasing RH levels: 9%, 22%, 33%, 58%, 75%, 84% and 97%, which were created by using different saturated salt solutions: KOH, CH$_3$CO$_2$K, MgCl$_2$, NaBr, NaCl, KCl and K$_2$SO$_4$, respectively. Samples were considered to be in equilibrium with the environment when a constant mass was reached. Temperature was kept constant at 30°C throughout the test. RH levels were monitored with hygrometer sensors (HygroPuce, Waranet Solutions, France) (Arrigoni et al., 2017).

1.5. Catalyst structure analysis

BET (Brunauer–Emmett–Teller) specific surface area, pore size and pore volume distribution for different catalysts were determined by nitrogen adsorption–desorption isotherms, which were measured at −196°C (ASAP2020, Micromeritics, USA). Prior to the measurements, a sample (~0.2 g) was pretreated with a temperature of 100°C in a vacuum system for 24 hr. The BET equation (relative pressure between 0.05 and 0.35) was employed to calculate the specific surface areas. Pore size and pore volume distributions were calculated from the adsorption branches of nitrogen physisorption isotherms and the DFT (density functional theory) method (Jagiello et al., 2007).

2. Results and discussion

To compare the decomposition performance of different catalysts, removal efficiencies ORE and NRE were defined as follows:

$$ORE\ (\%) = \frac{[O_3]_{inlet} - [O_3]_{outlet}}{[O_3]_{inlet}} \times 100\%$$

$$NRE\ (\%) = \frac{[NO_2]_{inlet} - [NO_2]_{outlet}}{[NO_2]_{inlet}} \times 100\%$$

where $[O_3]_{inlet}$, $[O_3]_{outlet}$, $[NO_2]_{inlet}$ and $[NO_2]_{outlet}$ are the average concentration (mol/m^3) of O$_3$ and NO$_2$ at the inlet and at the outlet, respectively, of the FCR, of which $[O_3]_{outlet}$ and $[NO_2]_{outlet}$ were based on an average of the last 10 min of the testing time.

The O$_3$ degradation rate (ODR) and NO$_x$ degradation rate (NDR) (mol/(sec·g$_{cat}$)) were defined as:

$$ODR = \frac{([O_3]_{inlet} - [O_3]_{outlet}) \times Q_{flow}}{m_{cat}}$$

$$NDR = \frac{([NO_2]_{inlet} - [NO_2]_{outlet}) \times Q_{flow}}{m_{cat}}$$

where Q_{flow} (m^3/sec) is the gas flow rate in FCR and m_{cat} (g) is the catalyst mass.

2.1. Catalyst decomposition performance

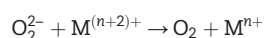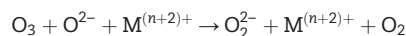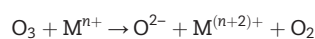#### 2.1.1. Effect of precursor kind and percentage
According to the literature, the different kinds and percentages of precursor used for supported transition metal oxide catalysts could influence the dispersion of the precursor on the support and the decomposition performance of the catalyst (Heisig et al., 1997; Rezaei et al., 2013). Therefore, it is necessary to investigate the effect of the precursor percentage for different

catalysts on the O$_3$ and NO$_2$ removal efficiency. Fig. 5 shows the removal efficiency in FCR for 2 g γ-Al$_2$O$_3$ alone and 2 g 1, 5 and 10 wt.% of NiO$_x$/Al$_2$O$_3$, CoO$_x$/Al$_2$O$_3$ and MnO$_x$/Al$_2$O$_3$ catalysts at RH < 2%, which was considered a dry condition in this study. As shown in Fig. 5a, ORE first increases and then decreases as the precursor percentage increases. It reaches the optimal value of 65% at 5 wt.% catalyst. However, the change of ORE is negligible between 1 and 5 wt.% CoO$_x$/Al$_2$O$_3$. This development in ORE is mainly due to the change in crystal form of the transition metal oxides and their loading amount on the support (Wang et al., 2014, 2016). With a lower loading amount, the principle morphology of deposited oxide is in the form of a porous lichen-like structure. While increasing the loading amount, the lichen-like structure collapses and forms a compact layer on the support (Wang et al., 2014), which can significantly decrease the specific surface area of the catalyst. In this study, the specific surface area of MnO$_x$/Al$_2$O$_3$ catalysts decreases from 240, 238 to 200 m^2/g as the precursor percentage increases from 1, 5 to 10 wt.%. A greater decrease in specific surface area signifies the formation of a more compact structure over the catalyst surface. Therefore, catalysts with 5 wt.% precursor show the best ORE, which is mainly attributed to their porous lichen-like structure and relatively high precursor loading amount. As a consequence, we suggest that the catalytic activity of a supported transition metal oxide catalyst for O$_3$ decomposition depends on a compromise between the specific surface area and the precursor loading amount. Moreover, about 10% and 40% of ORE and NRE, respectively, for γ-Al$_2$O$_3$ alone can be seen in Fig. 5. This could be due to the relatively high specific surface area (250 m^2/g) and the catalytic activity of γ-Al$_2$O$_3$ for O$_3$ and NO$_2$. The study of Dhandapani and Oyama (1997) proved this phenomenon. The authors obtained an ORE of 19% for γ-Al$_2$O$_3$ alone in the experimental conditions.

The catalytic mechanisms of the O$_3$ decomposition process on supported transition metal oxide catalysts were well established, as follows (Li et al., 1998):

$$O_3 + * \rightarrow O^* + O_2$$

$$O_3 + O^* \rightarrow O_2^* + O_2$$

$$O_2^* \rightarrow O_2 + *$$
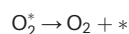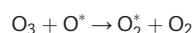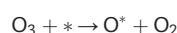
where * denotes an active site on the catalyst surface. Moreover, Radhakrishnan and Oyama (2001b) suggested that O$_3$ decomposition over MnO$_x$/Al$_2$O$_3$ catalyst proceeds through an electron transfer from the Mn site to the O$_3$ molecule, and Mn is reduced when the oxygen species desorb from the catalyst surface. A similar phenomenon was also observed for other metal oxides (e.g., FeO catalyst) or noble metals (e.g., Pd) (Tidahy et al., 2007). Therefore, a new mechanism for O$_3$ decomposition on supported transition metal oxide catalysts is proposed:

$$O_3 + M^{n+} \rightarrow O^{2-} + M^{(n+2)+} + O_2$$

$$O_3 + O^{2-} + M^{(n+2)+} \rightarrow O_2^{2-} + M^{(n+2)+} + O_2$$

$$O_2^{2-} + M^{(n+2)+} \rightarrow O_2 + M^{n+}$$

with M the transition metal such as Ni, Co and Mn.

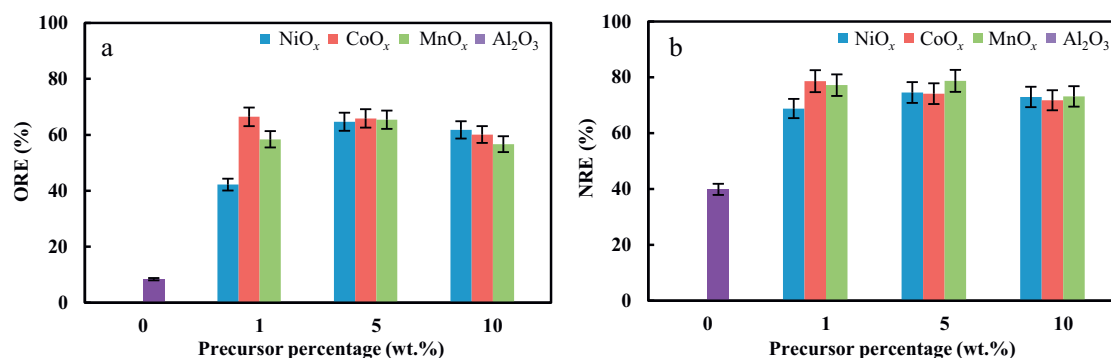For NO$_x$ removal, Fig. 5b shows that NRE varies from 70% to 80% for all catalysts, except for 1 wt.% NiO$_x$/Al$_2$O$_3$, whose NRE

Fig. 5 – (a) O_3 removal efficiency (ORE) and (b) NO_2 removal efficiency (NRE) in fixed-bed catalytic reactor (FCR) on 2 g catalysts and γ-Al_2O_3 alone in dry conditions (RH < 2%).

is 69%. Furthermore, 5 wt.% MnO_x/Al_2O_3 has the highest NRE of 79%. This small difference of NRE is probably due to the relatively low concentration of NO_2 compared with that of O_3, which signifies a relatively small dependence of precursor loading amount for NO_2 decomposition. Besides, no NO was detected at the outlet of the FCR in all the experiments. Many studies have investigated the NO_x decomposition mechanisms over supported transition metal oxide catalysts. Lin et al. (2016) proposed a mechanism for the catalytic deep oxidation of NO_x by O_3 over MnO_x/Al_2O_3 catalyst. In the first step, O_3 is decomposed into active oxygen atoms on the catalyst surface; then, manganese is oxidized into manganese (IV) and manganese(VII) via the decomposition of O_3. Subsequently, NO_2 adsorbed on the catalyst surface is oxidized by active oxygen atoms or oxidized manganese ions, generating NO_3 and nitrates. Finally, N_2O_5, formed by the combination of NO_2 and NO_3, is desorbed from the catalyst surface. Based on this mechanism, a simpler one, which skips the intermediates and finally forms nitrogen, is proposed in this study:

$$NO_2 + 2* \rightarrow NO_2^{**}$$

$$2NO_2^{**} \rightarrow N_2^{**} + 2O_2^*$$

$$O_2^* \rightarrow O_2 + *$$

$$N_2^{**} \rightarrow N_2 + 2*$$
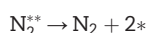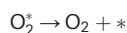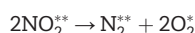
2.1.2. Effect of relative humidity

Given the intended application of the prepared catalysts for indoor air treatment, the influence of humid conditions is unavoidable, since a RH between 40% and 65% is mostly encountered in indoor environments (Kirchner et al., 2006) and considered comfortable for humans (Fauconnier, 1992). Therefore, the effects of different RH on ORE and NRE for 5 wt. % catalysts in humid conditions were investigated. As seen in Fig. 6a, ORE dramatically decreases with increasing RH from <2% to 60%. For example, the ORE of MnO_x/Al_2O_3 is 65% in dry conditions; it decreases to 26%, 20% and 20% when RH increases to 20%, 40% and 60%, respectively. The same behavior is also observed for NRE, as indicated in Fig. 6b. Besides, the effect of RH on ORE for CoO_x/Al_2O_3 seems less important than that of NiO_x/Al_2O_3 and MnO_x/Al_2O_3 at a low RH: ORE decreases from 66% to 39% when RH increases from <2% to 20% for CoO_x/Al_2O_3, while the ORE changes from 65% to 28% and 65% to 26% for NiO_x/Al_2O_3 and MnO_x/Al_2O_3, respectively, for the same change in RH. Furthermore, CoO_x/Al_2O_3 and MnO_x/Al_2O_3 present a better ORE at high RH: about 20% for CoO_x/Al_2O_3 and MnO_x/Al_2O_3 compared with 10% for NiO_x/Al_2O_3 at 60% RH. Moreover, at a relatively high RH (40% to 60%), the change in RH has little influence on ORE for MnO_x/Al_2O_3: ORE remains at about 20% as RH increases from 40% to 60%, while that for NiO_x/Al_2O_3 and CoO_x/Al_2O_3 decreases from 21% to 10% and from 26% to 20%, respectively.
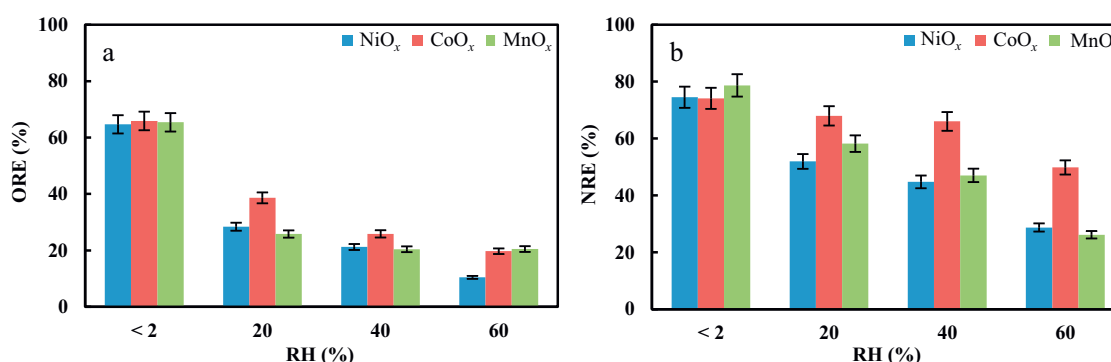

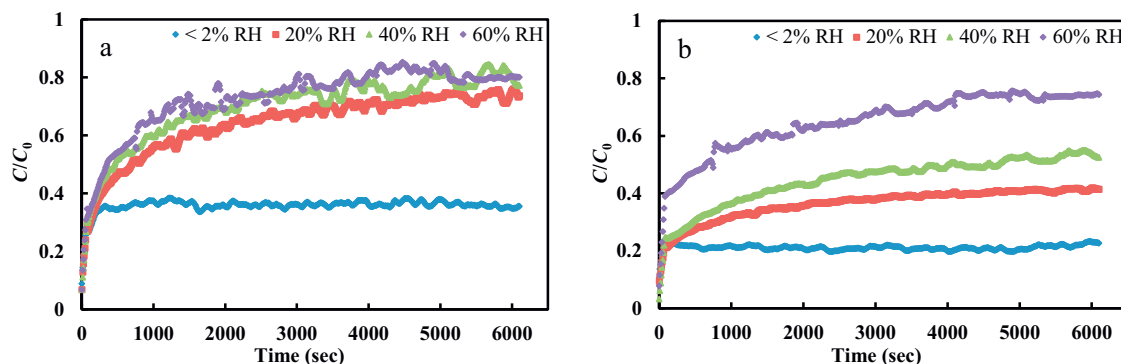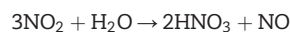**Fig. 6 – (a) ORE and (b) NRE in FCR on 2 g 5 wt.% catalysts at different RH levels.**

Fig. 7 – Time profiles for dimensionless concentration (C/C_0) for (a) O_3 and (b) NO_2 in FCR on 2 g 5 wt.% MnO_x/Al_2O_3 catalyst at different RH levels.

These results indicate that the catalytic activity of MnO_x/Al_2O_3 is relatively stable for O_3 decomposition at a relatively high RH. For the effect of RH on NO_2 removal, as seen in Fig. 5b, CoO_x/Al_2O_3 shows a better NRE than that of NiO_x/Al_2O_3 and MnO_x/Al_2O_3 as RH increases. Thus, we conclude that the catalytic activity of CoO_x/Al_2O_3 for NO_2 decomposition in the presence of water vapor is better than that of the other tested catalysts.

Fig. 7 illustrates the progression of the ratio between outlet concentration and inlet concentration of O_3 and NO_2 in the FCR for 2 g 5 wt.% MnO_x/Al_2O_3 catalyst at different RH levels. For both O_3 and NO_2, the outlet concentration clearly increases as the RH increases. As stated previously, the decrease in catalytic activity for O_3 and NO_2 decomposition at higher RH could be attributed to the competitive adsorption between water vapor molecules and O_3, NO_2 molecules over the active sites of the catalyst. Because of the hydrophilicity of Al_2O_3, water molecules are relatively easier to be adsorbed on the catalyst surface than other molecules. They thus cover the catalyst by occupying the active sites. In this way, water molecules prevent the contact of other molecules with the catalyst surface, thereby reducing the catalytic decomposition performance for O_3 and NO_2. Moreover, Rakitskaya et al. (1999) proved that catalysts with increasing amounts of absorbed water show a decreasing catalytic activity for O_3 decomposition.

As seen in Fig. 8, which presents the ORE and NRE for 1, 5 and 10 wt.% MnO_x/Al_2O_3 catalysts and γ-Al_2O_3 alone at 60% RH, ORE and NRE decrease slightly while the precursor percentage increases. This result is probably attributed to the increase of hydrophilicity of the catalyst surface. As expected, oxygen is the second most electronegative element, which can attract other electrons to itself in a covalent bond, because of its solitary electrons. In this way, a hydrogen bond can be easily formed between an oxygen atom and a hydrogen atom provided by water molecules. Therefore, as the precursor percentage increased, more manganese oxides were deposited over the catalyst, which introduced more oxygen atoms and thus led to an increase in the hydrophilicity of the catalyst surface. The more hydrophilic the catalyst surface is, the easier the adsorption of water molecules becomes. As a result, less O_3 and NO_2 was adsorbed on the catalyst surface and the removal efficiency thus decreased. In addition, in contrast to the negligible ORE for γ-Al_2O_3 alone, about 20% of NRE was observed. The presence of water enhances the oxidation of NO_2 since the formation of nitric acid is possible (Ortiz et al., 2000):

$$3NO_2 + H_2O \rightarrow 2HNO_3 + NO$$

Besides, this phenomenon is also probably due to the degradation of NO_2 in the presence of γ-Al_2O_3 under reaction
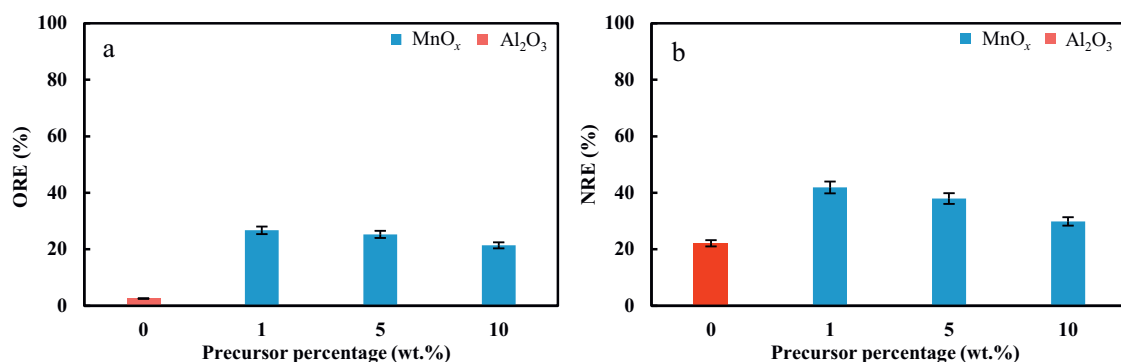

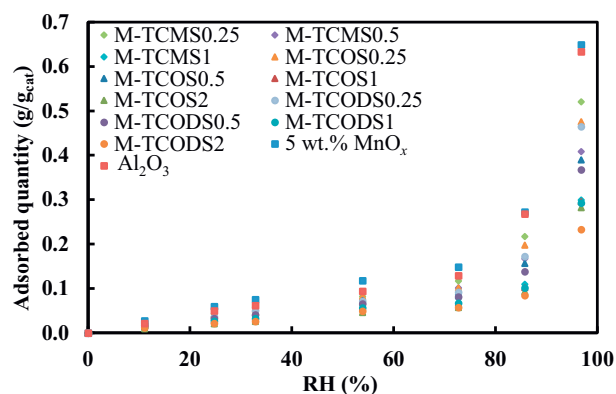**Fig. 8 – (a) ORE and (b) NRE in FCR on 2 g MnO_x/Al_2O_3 catalysts and γ-Al_2O_3 alone at 60% RH.**

Fig. 9 – Adsorption isotherms of surface-modified, non-modified catalysts and γ-Al₂O₃ alone. MnOₓ/Al₂O₃ surface-modified catalysts with different grafted modifying agents are denoted as M-modifying agent-Q. Modifying agents are TCMS, TCOS and TCODS, and the ratios (Q) of modifying agent to the amount of 5 wt.% MnOₓ/Al₂O₃ catalyst are 0.25, 0.5, 1 and 2 mmol/gcat.

with O₃, such as the reaction proposed below. However, this is only a preliminary suggestion. The mechanism, the intermediates and the feasibility of this reaction will be studied in subsequent research.

$$O_3 + 6NO_2 + Al_2O_3 + nH_2O \rightarrow 2Al(NO_3)_3 \cdot nH_2O$$
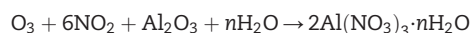
Although CoOₓ/Al₂O₃ catalyst showed good performance in both O₃ and NO₂ decomposition, its practical application is limited due to the toxicity. According to the International Agency for Research on Cancer (IARC), metallic cobalt and cobalt compounds have been classified as "potential carcinogenic" to humans (Group 2B, IARC) since 1991 (revised 2006) for inhalation exposure (World Health Organization et al., 2006). In addition, a minor difference in ORE for the three 5 wt.% catalysts was also observed. This result made it possible to focus on the 5 wt.% MnOₓ/Al₂O₃ catalyst for the following studies.

2.2. Comparison between different surface-modified catalysts

As mentioned previously, the supported transition metal oxide catalysts used in this study were hydrophilic. This is mainly due to the presence of hydroxyl groups on the γ-Al₂O₃ surface and oxygen atoms introduced by the deposited metal oxides. Experimental results showed strongly negative effects of RH on the catalytic decomposition performance for O₃ and NO₂. In order to overcome this limitation, the 5 wt.% MnOₓ/Al₂O₃ catalyst was modified by a cost-effective chemical grafting method to make it hydrophobic. In this part of the study, we investigated the effects of different linker lengths and amounts of modifying agent on the hydrophobicity and the

decomposition performance between different surface-modified catalysts.

2.2.1. Adsorption isotherm
As seen in Fig. 9, the adsorption isotherms of surface-modified, non-modified catalysts and γ-Al₂O₃ alone are similar to the type-IV adsorption isotherm according to the International Union of Pure and Applied Chemistry (IUPAC) classification (Sing et al., 1984). The adsorbed water quantity for the 5 wt.% MnOₓ/Al₂O₃ non-modified catalyst is slightly higher than that of γ-Al₂O₃ alone. This result proves that the 5 wt.% MnOₓ/Al₂O₃ non-modified catalyst is more hydrophilic than the γ-Al₂O₃ alone, because of the additional oxygen atoms introduced by the deposited manganese oxide. Moreover, surface-modified catalysts show a smaller capacity for water adsorption: their maximum adsorbed water quantity is about two thirds of that for the non-modified catalyst, which means that the hydrophilicity of the 5 wt.% MnOₓ/Al₂O₃ catalyst was greatly changed by the surface modification treatment. As expected, the aliphatic hydrocarbon substituents of TCAS are of a hydrophobic nature. Owing to the surface modification process, they were grafted on the catalyst surface, of which the character thus changed to hydrophobic. Furthermore, among the surface-modified catalysts, an obvious decrease in adsorbed water quantity with the increase in the linker length and in the amount of modifying agent, especially at a high RH level, was observed. This observation is attributed to the improvement of the hydrophobicity of the surface-modified catalysts. In fact, with a longer linker and a greater amount of modifying agent, the hydrophobicity of the catalyst surface can be greatly improved. The same results have also been obtained by other authors (Esmaeilirad et al., 2016), whose study was based on the substrate of aluminum alloy.

2.2.2. BET and DFT analysis
The BET specific surface area and pore volume distribution for different catalysts, as well as γ-Al₂O₃ alone, are summarized in Table 1. It is worth noting that there are few micropores (pore width < 2 nm) in the catalysts, since the volume of micropores is much smaller than that of the mesopores (pore width from 2 to 50 nm). We found that with an increasing amount of modifying agent, the specific surface area evidently decreases, as does the volume of pores. For example, the specific surface area of surface-modified catalysts decreased from 232, 207 to 138 m²/g as the ratio Q of TCOS increased from 0.25, 0.5 to 1 mmol/gcat, respectively, compared with that of 240 m²/g for the non-modified catalyst and 250 m²/g for γ-Al₂O₃ alone. The same decreasing tendency could be deduced for other modifying agents of TCAS.

2.2.3. Catalytic decomposition performance at 60% RH
As mentioned in the previous section, RH has a strongly negative effect on the catalytic decomposition performance of

Table 1 – BET (Brunauer–Emmett–Teller) specific surface area and pore volume distribution.					
	γ-Al₂O₃	5 wt.% MnOₓ/Al₂O₃	M-TCOS0.25	M-TCOS0.5	M-TCOS1
BET (m²/g)	250	240	232	207	138
Volume of micropores (cm³/g)	0.006	0.004	0.001	0.001	0.001
Volume of mesopores (cm³/g)	0.640	0.586	0.542	0.486	0.322

O_3 and NO_2: for the 5 wt.% MnO_x/Al_2O_3 non-modified catalyst, the ORE and NRE decrease from 65% to 20% and 79% to 26%, respectively, when RH increases from <2% to 60%. In this section, the catalytic decomposition performance of 5 wt.% MnO_x/Al_2O_3 surface-modified catalysts for O_3 and NO_2 at 60% RH will be investigated. The ORE and NRE for 2 g surface-modified catalysts by different linker lengths and amounts of TCAS at 60% RH are presented in Fig. 10, along with the values for the non-modified catalyst. A clear decreasing tendency for ORE is noted as the linker length and amount of TCAS increases. In particular, this decreasing tendency is more obvious for the TCAS with a longer linker. As the ratio Q increases from 0.25 to 1 mmol/g_{cat}, the ORE decreases from 41% to 35%, 40% to 31% and 40% to 22% for M-TCMS, M-TCOS and M-TCODS, respectively, as summarized in Table 2, as well as for ODR, NRE and NDR. These results show the negative effect of linker length and amount of modifying agent on the catalytic decomposition performance. This is probably attributed to the decrease in catalytic activity of the catalyst surface and the increase in steric hindrance effect. In other words, a higher specific surface area signifies a higher dispersion of active components over the catalyst surface and a larger contact area between the active components and gas molecules, which can lead to a better catalytic activity (Guo et al., 2007). However, as shown in Table 1, a greater amount of modifying agent resulted in a smaller specific surface area and led to pores clogging, since the volume of the pores decreased. Moreover, as the linker length and amount of TCAS increase, the longer and greater amount of aliphatic hydrocarbon substituents will potentially increase the steric hindrance effect on the catalyst surface. This means that the access of O_3 molecules to the catalyst surface and into the pores is significantly more difficult, as well as other molecules such as NO_2. Overall, the longer the linker, the more significant the steric hindrance effect. This is the reason for the more obvious ORE decrease tendency of the modifying agent with a longer linker. As seen from the time profiles for the dimensionless concentration of O_3 in Fig. 11, the increase in the linker length and in the amount of modifying agent can effectively augment the O_3 concentration at the outlet of the FCR, which signifies a decrease in ORE. Although a higher linker length and a greater amount of modifying agent can greatly improve the hydrophobicity of the catalyst surface, it can negatively influence

Table 2 – Summary of the removal efficiency and degradation rate of O_3 and NO_2 for different catalysts at 60% RH.

Material	ORE (%)	ODR (10^{-10} mol/(sec·g_{cat}))	NRE (%)	NDR (10^{-10} mol/(sec·g_{cat}))
5 wt.% NiO_x/Al_2O_3	10	11.6	29	1.5
5 wt.% CoO_x/Al_2O_3	20	21.8	50	2.6
5 wt.% MnO_x/Al_2O_3	20	22.7	26	1.4
M-TCMS0.25	41	62.6	0[a]	0[a]
M-TCMS0.5	37	43.1	0[a]	0[a]
M-TCMS1	35	49.1	0[a]	0[a]
M-TCOS0.25	40	57.3	11	0.3
M-TCOS0.5	35	43.8	15	0.5
M-TCOS1	31	38.9	20	0.6
M-TCOS2	22	25.8	6	0.2
M-TCODS0.25	40	58.3	20	0.6
M-TCODS0.5	33	36.6	18	0.5
M-TCODS1	22	24.2	14	0.4
M-TCODS2	3	3.6	4	0.1

ODR: O_3 degradation rate; NDR: NO_x degradation rate.
[a] negligible NER and NDR, which are considered in the range of measurement uncertainty.

the catalytic activity at the same time. As a result, an optimal linker length and amount of modifying agent should be determined to improve the catalytic decomposition performance at high RH: to meet both the hydrophobicity of the catalyst, but also the catalytic activity. In the present study, the surface-modified catalyst with the shortest modifying agent of TCMS and the lowest ratio Q of 0.25 mmol/g_{cat} showed the best catalytic decomposition performance for O_3. Its ORE was 41% at 60% RH, which increased 21% more for the removal efficiency compared with that of the non-modified one. In addition, the difference in ORE between the surface-modified catalysts with ratio Q of 0.25 mmol/g_{cat} was small: 41%, 40% and 40% for M-TCMS0.25, M-TCOS0.25 and M-TCODS0.25, respectively.

In contrast to the ORE, a lower NRE can be observed for the surface-modified catalysts in Fig. 10b. This phenomenon could be explained by the negative influence of the steric hindrance effect on NO_2 decomposition. As previously presented, the concentration of NO_2 is much lower than that of
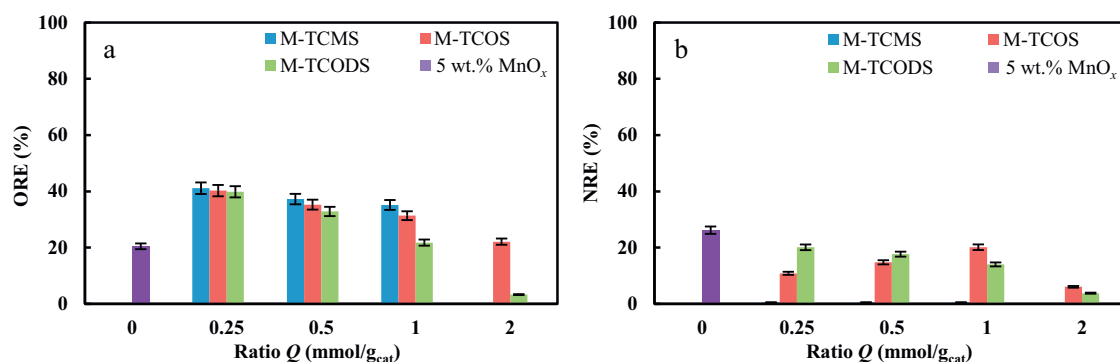

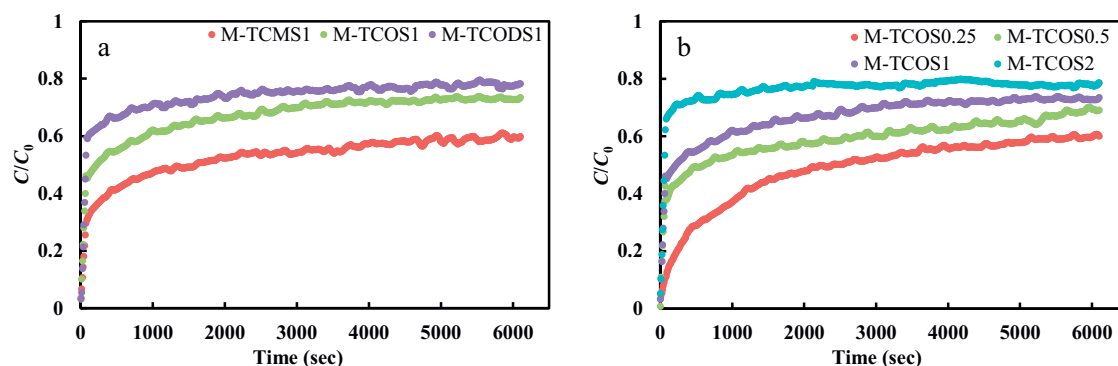Fig. 10 – (a) ORE and (b) NRE in FCR on 2 g 5 wt.% MnO_x/Al_2O_3 non-modified and surface-modified catalysts at 60% RH.

Fig. 11 – Effects of (a) linker length and (b) modifying agent amount on time profiles for dimensionless concentration in FCR on 2 g 5 wt.% MnO_x/Al_2O_3 surface-modified catalysts at 60% RH.

O_3 at the inlet of the FCR, as well as that of water molecules in humid conditions. A lower concentration results in a relatively lower partial pressure of NO_2. Besides, modifying agents that are introduced on the surface-modified catalysts could potentially lead to a steric hindrance effect. When competitive adsorption occurs among molecules, a lower NO_2 partial pressure means fewer NO_2 molecules can access the catalyst surface, especially in the presence of the steric hindrance effect, which can further prevent the contact of NO_2 molecules with the catalyst surface. Therefore, a lower NRE was obtained. A negligible NRE for the M-TCMS surface-modified catalyst is shown in Fig. 10b, which is considered in the range of measurement uncertainty. Furthermore, the M-TCODS0.25 catalyst has the best decomposition performance for NO_2, with an NRE of 20%.

3. Conclusions

In the present work, a series of supported transition metal oxide catalysts were prepared *via* vacuum impregnation method for the decomposition of O_3 and NO_2, which are considered toxic by-products formed in NTP. The effects of precursor percentages of different catalysts on O_3 and NO_2 removal efficiency were investigated, as well as for different RH. The results showed strong negative effects of RH on the catalytic decomposition performance. Subsequently, a cost-effective chemical grafting method was carried out by impregnating the 5 wt.% MnO_x/Al_2O_3 catalyst with different modifying agents of TCAS, in order to improve the hydrophobicity of the catalyst surface and the catalytic activity at high RH. The following conclusions can be drawn from the results of the present study:

(1) In dry conditions, catalysts prepared with a 5 wt.% precursor show the best catalytic activity, attributed to their relatively high specific surface area and precursor loading amount. A negligible difference was observed between ORE and NRE for 5 wt.% of NiO_x/Al_2O_3, CoO_x/Al_2O_3 and MnO_x/Al_2O_3 catalysts.

(2) When RH increases from <2% to 20%, ORE and NRE dramatically decrease, which is due to the competitive adsorption with water molecules. As RH continues to increase, the catalytic activity of MnO_x/Al_2O_3 remains relatively stable for O_3 decomposition and CoO_x/Al_2O_3 presents a better NRE than the other catalysts. This finding provides an alternative of the binary oxide MnO_x-CoO_x catalyst for the following research, which could simultaneously improve the catalytic activity for O_3 and NO_2 decomposition.

(3) The surface modification treatment can greatly improve the hydrophobicity of the 5 wt.% MnO_x/Al_2O_3 catalyst and the decomposition performance for O_3. The surface-modified catalyst with the shortest modifying agent of TCMS and the lowest ratio Q of 0.25 mmol/g_{cat} shows the best catalytic decomposition performance for O_3, with an ORE of 41% at 60% RH, which increased by a further 21% for the removal efficiency compared with that of the non-modified catalyst.

(4) However, a lower NRE was observed for surface-modified catalysts compared with that of the non-modified one. This result could be attributed to the negative influence of the steric hindrance effect on NO_2 decomposition. The M-TCODS0.25 catalyst shows the best catalytic decomposition performance for NO_2. Thus, combination of the M-TCMS0.25 and the M-TCODS0.25 surface-modified catalysts can be considered a choice for further investigation of the NTP-catalysis processes for indoor air treatment.

In general, for a RH between 40% and 60%, which is close to the conventional conditions of the mostly encountered indoor environments, an optimum amount (*e.g.*, 0.25 mmol/g_{cat}) of TCAS can show the best catalytic decomposition performance and ensure a certain degree of hydrophobicity for the surface-modified catalysts. Further investigations will follow the effect of this amount of TCAS for lower or higher RH in order to obtain more information on the catalytic decomposition performance.

Acknowledgments

grateful to Laurent Duclaux and Laurence Reinert (LCME, Université Savoie Mont Blanc, France) for their helpful suggestions and technical support for the catalyst preparation.

REFERENCES

Arrigoni, A., Grillet, A.C., Pelosato, R., Dotelli, G., Beckett, C.T.S., Woloszyn, M., et al., 2017. Reduction of rammed earth's hygroscopic performance under stabilisation: an experimental investigation. Build. Environ. 115, 358–367.

Byeon, J.H., Park, J.H., Jo, Y.S., Yoon, K.Y., Hwang, J., 2010. Removal of gaseous toluene and submicron aerosol particles using a dielectric barrier discharge reactor. J. Hazard. Mater. 175, 417–422.

Carver, R.M., Zhang, J.S., Wang, Z., 2010. Air cleaning technologies for indoor air quality (ACT-IAQ): growing fresh and clean air.

Dhandapani, B., Oyama, S.T., 1997. Review: gas phase ozone decomposition catalysts. Appl. Catal. B Environ. 11, 129–166.

Einaga, H., Futamura, S., 2006. Effect of water vapor on catalytic oxidation of benzene with ozone on alumina-supported manganese oxides. J. Catal. 243, 446–450.

Esmaeilirad, A., Rukosuyev, M.V., Jun, M.B.G., van Veggel, F.C.J.M., 2016. A cost-effective method to create physically and thermally stable and storable super-hydrophobic aluminum alloy surfaces. Surf. Coat. Technol. 285, 227–234.

Everaert, K., Baeyens, J., 2004. Catalytic combustion of volatile organic compounds. J. Hazard. Mater. 109, 113–139.

Fan, X., Zhu, T., Wan, Y., Yan, X., 2010. Effects of humidity on the plasma-catalytic removal of low-concentration BTX in air. J. Hazard. Mater. 180, 616–621.

Fauconnier, R., 1992. L'action de l'humidité de l'air sur la santé dans les bâtiments tertiaires. Chauff. Vent. Cond..

Guo, Y., Ye, D., Chen, K., He, J., 2007. Toluene removal by a DBD-type plasma combined with metal oxides catalysts supported by nickel foam. Catal. Today 126, 328–337.

Guo, Y.F., Ye, D.Q., Chen, K.F., He, J.C., Chen, W.L., 2006. Toluene decomposition using a wire-plate dielectric barrier discharge reactor with manganese oxide catalyst in situ. J. Mol. Catal. A Chem. 245, 93–100.

Heisig, C., Zhang, W., Oyama, S.T., 1997. Decomposition of ozone using carbon-supported metal oxide catalysts. Appl. Catal. B Environ. 14, 117–129.

ISO, 2013. ISO 12571, 2013. Hygrothermal Performance of Building Materials and Products — Determination of Hygroscopic Sorption Properties.

Jagiello, J., Ania, C.O., Parra, J.B., Jagiello, L., Pis, J.J., 2007. Using DFT analysis of adsorption data of multiple gases including H_2 for the comprehensive characterization of microporous carbons. Carbon 45, 1066–1071.

Kirchner, S., Arenes, J.F., Cochet, C., 2006. Campagne nationale Logements: Etat de la qualité de l'air dans les logements français-Rapport final.

Kujawa, J., Cerneaux, S., Kujawski, W., 2014. Characterization of the surface modification process of Al_2O_3, TiO_2 and ZrO_2 powders by PFAS molecules. Colloids Surf. A Physicochem. Eng. Asp. 447, 14–22.

Kujawa, J., Cerneaux, S., Kujawski, W., 2015. Highly hydrophobic ceramic membranes applied to the removal of volatile organic compounds in pervaporation. Chem. Eng. J. 260, 43–54.

Kujawa, J., Kujawski, W., Koter, S., Rozicka, A., Cerneaux, S., Persin, M., et al., 2013. Efficiency of grafting of Al_2O_3, TiO_2 and ZrO_2 powders by perfluoroalkylsilanes. Colloids Surf. A Physicochem. Eng. Asp. 420, 64–73.

Li, W., Gibbs, G.V., Oyama, S.T., 1998. Mechanism of ozone decomposition on a manganese oxide catalyst. 1. In situ raman spectroscopy and ab initio molecular orbital calculations. J. Am. Chem. Soc. 120, 9041–9046.

Li, X., Wang, L., Xia, Q., Liu, Z., Li, Z., 2011. Catalytic oxidation of toluene over copper and manganese based catalysts: effect of water vapor. Catal. Commun. 14, 15–19.

Lin, F., Wang, Z., Ma, Q., Yang, Y., Whiddon, R., Zhu, Y., et al., 2016. Catalytic deep oxidation of NO by ozone over MnO_x loaded spherical alumina catalyst. Appl. Catal. B Environ. 198, 100–111.

Long, L., Zhao, J., Yang, L., Fu, M., Wu, J., Huang, B., et al., 2011. Room temperature catalytic ozonation of toluene over MnO_2/Al_2O_3. Chin. J. Catal. 32, 904–916.

Magureanu, M., Mandache, N.B., Eloy, P., Gaigneaux, E.M., Parvulescu, V.I., 2005. Plasma-assisted catalysis for volatile organic compounds abatement. Appl. Catal. B Environ. 61, 12–20.

Mista, W., Kacprzyk, R., 2008. Decomposition of toluene using non-thermal plasma reactor at room temperature. Catal. Today 137, 345–349.

Niu, J., Yang, X., Zhu, A., Shi, L., Sun, Q., Xu, Y., et al., 2006. Plasma-assisted selective catalytic reduction of NO_x by C_2H_2 over Co-HZSM-5 catalyst. Catal. Commun. 7, 297–301.

Ondarts, M., Hajji, W., Outin, J., Bejat, T., Gonze, E., 2017. Non-thermal plasma for indoor air treatment: toluene degradation in a corona discharge at ppbv levels. Chem. Eng. Res. Des. 118, 194–205.

Ortiz, A., Alonso, J.C., Pankov, V., Huanosta, A., Andrade, E., 2000. Characterization of amorphous aluminum oxide films prepared by the pyrosol process. Thin Solid Films 368, 74–79.

Paul, B., Martens, W.N., Frost, R.L., 2011. Surface modification of alumina nanofibres for the selective adsorption of alachlor and imazaquin herbicides. J. Colloid Interface Sci. 360, 132–138.

Qualité de l'air intérieur, ANSES. Available: https://www.anses.fr/fr/content/qualité-de-l'air-intérieur, Accessed September 3, 2016.

Radhakrishnan, R., Oyama, S.T., 2001a. Ozone decomposition over manganese oxide supported on ZrO_2 and TiO_2: a kinetic study using in situ laser Raman spectroscopy. J. Catal. 199, 282–290.

Radhakrishnan, R., Oyama, S.T., 2001b. Electron transfer effects in ozone decomposition on supported manganese oxide. J. Phys. Chem. B 105, 4245–4253.

Rakitskaya, T.L., Ennan, A.A., Granatyuk, I.V., 1999. Kinetics and mechanism of low-temperature ozone decomposition by co-ions adsorbed on silica. Catal. Today 53, 715–723.

Rezaei, E., Soltan, J., 2012. Low temperature oxidation of toluene by ozone over MnO_x/γ-alumina and $MnO_x/MCM-41$ catalysts. Chem. Eng. J. 198–199, 482–490.

Rezaei, E., Soltan, J., Chen, N., 2013. Catalytic oxidation of toluene by ozone over alumina supported manganese oxides: effect of catalyst loading. Appl. Catal. B Environ. 136–137, 239–247.

Sing, K.S.W., Everette, D.H., Haul, R.A.W., Moscou, L., Pierotti, R.A., Rouquérol, J., et al., 1984. Reporting physisorption data for gas solid systems with special reference to the determination of surface area and porosity. Pure Appl. Chem. 57, 603–619.

Subrahmanyam, C., Magureanu, M., Renken, A., Kiwi-Minsker, L., 2006. Catalytic abatement of volatile organic compounds assisted by non-thermal plasma. Appl. Catal. B Environ. 65, 150–156.

Thevenet, F., Sivachandiran, L., Guaitella, O., Barakat, C., Rousseau, A., 2014. Plasma–catalyst coupling for volatile organic compound removal and indoor air treatment: a review. J. Phys. D. Appl. Phys. 47, 224011.

Tidahy, H.L., Siffert, S., Wyrwalski, F., Lamonier, J.-F., Aboukaïs, A., 2007. Catalytic activity of copper and palladium based catalysts for toluene total oxidation. Catal. Today 119, 317–320.

Van Durme, J., Dewulf, J., Demeestere, K., Leys, C., Van Langenhove, H., 2009. Post-plasma catalytic technology for the removal of toluene from indoor air: effect of humidity. Appl. Catal. B Environ. 87, 78–83.

Van Durme, J., Dewulf, J., Leys, C., Van Langenhove, H., 2008. Combining non-thermal plasma with heterogeneous catalysis in waste gas treatment: a review. Appl. Catal. B Environ. 78, 324–333.

Van Durme, J., Dewulf, J., Sysmans, W., Leys, C., Van Langenhove, H., 2007. Efficient toluene abatement in indoor air by a plasma catalytic hybrid system. Appl. Catal. B Environ. 74, 161–169.

Wang, L., He, H., Zhang, C., Wang, Y., Zhang, B., 2016. Effets of precursors for manganese-loaded Al_2O_3 catalysts on plasma-catalytic removal of o-xylene. Chem. Eng. J. 406–413.

Wang, M., Zhang, P., Li, J., Jiang, C., 2014. The effects of Mn loading on the structure and ozone decomposition activity of MnO_x supported on activated carbon. Chin. J. Catal. 35, 335–341.

World Health Organization (Ed.), 2000. Air Quality Guidelines for Europe, 2nd ed. WHO regional publications. World Health Organization, Regional Office for Europe, Copenhagen.

World Health Organization, International Agency for Research on Cancer, IARC Working Group on the Evaluation of Carcinogenic Risks to Humans, 2006. Cobalt in Hard Metals and Cobalt Sulfate, Gallium Arsenide, Indium Phosphide, and Vanadium Pentoxide, IARC Monographs on the Evaluation of Carcinogenic Risks to Humans. International Agency for Research on Cancer; Distributed by WHO Press, Lyon, France: Geneva, Switzerland.